Temperature Dependence of Electron and Hole Impact Ionization Coefficients in GaN

Lina Cao, Zhongtao Zhu, Galen Harden, Hansheng Ye, *Graduate Student Member, IEEE*, Jingshan Wang, Anthony Hoffman, *Senior Member, IEEE*, and Patrick Fay, *Fellow, IEEE*

***Abstract*— The temperature dependence of the electron and hole impact ionization coefficients in GaN has been investigated experimentally. Two types of p-i-n diodes grown on bulk GaN substrates have been fabricated and characterized, and the impact ionization coefficients for both electrons and holes have been extracted using the photomultiplication method. Both the electron and hole impact ionization coefficients decrease as the temperature increases. The Okuto–Crowell model was used to describe the temperature dependence of the electron and hole impact ionization coefficients. Based on the measured impact ionization coefficients, the temperature dependence of the breakdown voltage of GaN non-punch through p-n diodes can be predicted; good agreement with experimentally reported results is obtained.**

***Index Terms*— GaN, impact ionization coefficients, non-punch through p-n diodes, temperature dependence.**

I. Introduction

GALLIUM nitride is very attractive for high power RF and mm-wave amplification and is emerging for lower frequency power conversion and control applications, due to its high mobility, high saturation velocity, and high critical electric field. The availability of high-quality bulk GaN substrates, in conjunction with improvements in material quality, impurity control, device design, and edge termination processes, has led to vertical devices capable of approaching the fundamental material limitations of GaN [1]–[4]. In this context, an improved understanding of impact ionization is needed in order to develop device designs and concepts that fully exploit the potential of GaN. In addition to optimizing the breakdown voltage (BV) of rectifiers and transistors, a full understanding of impact ionization is needed in order to harness the potential of less conventional devices, such as ultraviolet avalanche photodiodes (APDs) and high-power impact ionization transit-time (IMPATT) diodes.

Manuscript received July 11, 2020; revised October 2, 2020, November 24, 2020, January 1, 2021, and January 18, 2021; accepted January 20, 2021. Date of publication February 8, 2021; date of current version February 24, 2021. This work was supported by the U.S. Office of Naval Research (Paul Maki program manager) under Grant N00014-16-1-2850. The review of this article was arranged by Editor J. Mateos. *(Corresponding author: Patrick Fay.)*

Lina Cao, Zhongtao Zhu, Galen Harden, Hansheng Ye, Anthony Hoffman, and Patrick Fay are with the Department of Electrical Engineering, University of Notre Dame, Notre Dame, IN 46556 USA (e-mail: pfay@nd.edu).

Jingshan Wang is with Micron Technology Inc., Boise, ID 83707 USA.

Color versions of one or more figures in this article are available at https://doi.org/10.1109/TED.2021.3054355.

Digital Object Identifier 10.1109/TED.2021.3054355

Previously, very little experimental data on impact ionization in GaN were available, and much of what had been reported was on material with a high defect density grown on non-native substrates [5], [6]. Recently, impact ionization coefficients from devices fabricated on bulk GaN substrates have been reported [7]–[11]. Cao *et al.* [7], [8] have measured the electron and hole impact ionization coefficients using both wavelength-selective photomultiplication and noise spectral density measurements based on p-n junctions with a thin pseudomorphic $In_{0.07}Ga_{0.93}N$ layer grown on bulk GaN substrates, but no temperature dependence was reported. Ji *et al.* [9] obtained the impact ionization coefficients using the photomultiplication method based on p-on-n and n-on-p (with a buried p-GaN layer) diodes grown on bulk GaN substrates. However, the use of near bandgap illumination (350 nm) in this work leads to substantial photogeneration in the high-field region, complicating the analysis and potentially underestimating the extracted coefficients. Maeda *et al.* [10], [11] extracted the impact ionization coefficients utilizing the Franz–Keldysh effect based on the p^-/n^+ diodes grown on bulk GaN substrates. This approach requires additional assumptions, particularly about the optical absorption profile in the material. Temperature dependence was reported in [10] under the assumption that electrons and holes are symmetric (i.e., $\alpha = \beta$); the asymmetry was reported in [11] but without temperature dependence.

In this article, the impact ionization coefficients of electrons and holes in GaN were experimentally determined from 298 to 398 K using the photomultiplication method based on two p-i-n structures grown on bulk GaN substrates. The temperature dependence of the electron and hole impact ionization coefficients was modeled accurately using the Okuto–Crowell model. To validate the results, the measured characteristics are used to project the avalanche-limited performance limit for vertical devices and are compared against measured device results from the literature. The temperature dependence of the breakdown voltage of GaN nonpunchthrough p-n diodes has also been predicted and compared to experimental results.

II. Device Design and Fabrication

Fig. 1 shows a schematic cross section of the device structures used in this work. Fig. 1(a) shows the GaN p-i-n diode with a buried $In_{0.07}Ga_{0.93}N$ layer on the cathode side for hole injection studies. Grown on 2-in bulk GaN substrates by metal–organic chemical vapor deposition (MOCVD), the structure (from top to bottom)

This work is licensed under a Creative Commons Attribution 4.0 License. For more information, see https://creativecommons.org/licenses/by/4.0/

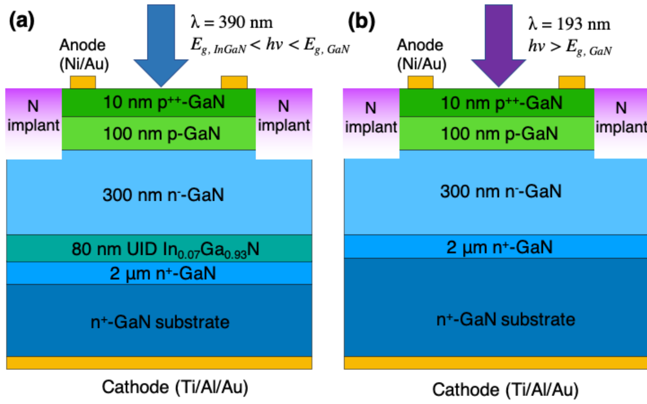

Fig. 1. Schematic cross section of the fabricated photodiodes: (a) p-i-n diode with a buried $In_{0.07}Ga_{0.93}N$ layer, designed for pure hole injection with 390-nm UV illumination; (b) p-i-n diode used for pure electron injection with 193-nm UV illumination.

consists of a 10-nm p^{++} contact layer, a 100-nm p-GaN layer (Mg: 2×10^{19} cm^{-3}), a 300-nm n-GaN drift layer (Si: 2×10^{16} cm^{-3}), an 80-nm undoped pseudomorphic $In_{0.07}Ga_{0.93}N$ layer, and 2-μm n^+-GaN layer (Si: 4×10^{18} cm^{-3}). The $In_{0.07}Ga_{0.93}N$ layer is used as a photoabsorption layer to produce pure hole injection under 390-nm UV illumination ($E_{g,\mathrm{InGaN}} < h\upsilon < E_{g,\mathrm{GaN}}$). The hole-initiated multiplication factors are obtained from reverse-bias photocurrent measurements of this structure. In this approach, hole-initiated avalanche can be studied without complications arising from activation of buried p-type layers or Mg diffusion into the drift layer [9].

However, the insertion of narrower bandgap InGaN layers in the structure leads to an increased dark current that makes measurement of the electron coefficients more challenging. In contrast to the case for holes, the low electron multiplication factor and small electron injection density partially obscure the photocurrent in the measurement, leading to appreciable scatter in the extracted electron impact ionization coefficients [7]. Therefore, we have also fabricated p-i-n diodes without an InGaN layer [see Fig. 1(b)] and extracted the electron impact ionization coefficients using this structure. This structure is nominally identical to the device shown in Fig. 1(a), except without the InGaN layer. Under 193-nm UV illumination ($h\upsilon > E_g$, GaN), a pure electron current is induced since the absorption coefficient of GaN at this wavelength is estimated to be 2.9×10^5 cm^{-1} and electron-initiated multiplication factors can be obtained (>96% of the incident light is absorbed in the 110-nm p-GaN anode layers) [12]. The use of this structure also avoids complications associated with Mg activation in buried p-type layers [9]. For both structures in Fig. 1, Ni/Au anode ohmic contacts to the p-GaN and Ti/Al/Au ohmic back cathode contacts were used. The top p-contact was ring-shaped to allow UV illumination. Edge termination with N ion implantation was used to suppress edge effects. The fabrication process details have been reported in [7].

III. Results and Discussion

Fig. 2(a) shows the measured reverse I–V curves of the devices with InGaN layer under dark and 390-nm UV illumination at 298, 348, and 398 K. Under illumination at this wavelength ($E_{\mathrm{g,\,InGaN}} < h\upsilon < E_{g,\mathrm{GaN}}$), electron–hole pairs are generated in the InGaN layer, and the holes are swept into the n^--GaN layer, resulting in pure hole injection into the drift layer. An optical intensity of 2 mW/cm^2, calibrated using a power meter, was used. To ensure that the photocurrent arises only from the InGaN layer, measurements of the photoresponse of the GaN-only structure in Fig. 1(b) under 390-nm illumination were performed. The measured photocurrent was on the order of 1000 times smaller than the InGaN-containing structures in Fig. 2(a), confirming pure hole injection conditions. As can be seen from Fig. 2(a), the device shows a positive temperature coefficient of breakdown voltage, a signature of avalanche breakdown. The dark currents (dashed lines) are much lower than the photocurrents (solid lines) when the reverse bias is higher than the flatband voltage (~40 V) of the polarization-induced barrier at the n^--GaN/InGaN interface. Above the flatband voltage of the polarization barrier, the photocurrent is dominated by holes injected from the InGaN into the n^--GaN layer. At lower applied voltages (<34 V, corresponding to electric fields below 1.1 MV/cm), the measured photocurrent is consistent with Franz–Keldysh absorption. For voltages above flatband, the photocurrent is nearly independent of temperature below breakdown as expected.

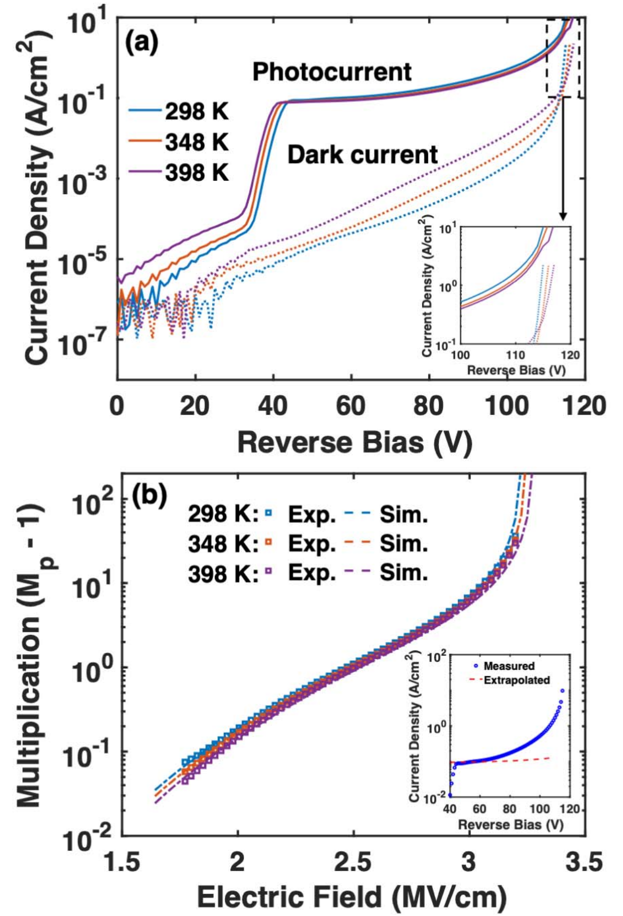

Fig. 2. (a) Reverse I–V curves of the devices with InGaN layer under dark and 390-nm UV illumination at various temperatures. Inset: expanded view in breakdown. (b) Electric field dependence of multiplication ($M_p - 1$) obtained from the above photocurrent measurements. Symbols show the experimental results, and dashed lines show the simulated values using ionization coefficients obtained here (as shown in Table I). Inset: measured photocurrent (∘) versus extrapolated photocurrent (–) at 298 K.

The small decrease in photocurrent at elevated temperature is believed to be due to reduced nonradiative recombination lifetime with increased temperature [13], [14]. In contrast, for the low-voltage range below flatband, larger photocurrents are observed at higher temperatures. This may be due to a combination of increased hole thermionic emission over the n^--GaN/InGaN barrier and enhanced sub-bandgap absorption at elevated temperatures.

When the reverse bias is raised above the flatband voltage of the n^--GaN/InGaN barrier, the photocurrent starts to increase due to avalanche multiplication. As shown by the inset of Fig. 2(b), the hole-initiated multiplication factors M_p are extracted as the ratio of the measured current under illumination (including amplification, shown by the blue circles) to the baseline photocurrent (red broken lines). Measurement of devices with different areas and as a function of bias (not shown) indicated that the reverse current followed a $\ln(J) \sim E$ trend, indicative of variable-range hopping dominated transport below the onset of avalanche [15]. Consequently, the baseline photocurrent was extrapolated into the avalanche region using $J_{\mathrm{ph},p} = J_0 + J_1 \exp(p_1 V)$, where $J_0 = 9.60 \times 10^{-2}$ A/cm^2 accounts for the photogenerated current and $J_1 = 8.64 \times 10^{-5}$ A/cm^2 and $p_1 = 5.49 \times 10^{-2}$ V^{-1} reflect the additional current contribution with increasing field for variable-range hopping conduction, as determined from least-squares fitting to the measured photocurrent from 45 to 55 V [15]–[17]. The hole-initiated multiplication factors are plotted as a function of the average electric field in the n^--GaN layer at different temperatures in Fig. 2(b). As can be seen, the breakdown voltage increases, and the multiplication factors decrease at elevated temperatures. Since the hole ionization coefficient is much larger than the electron ionization coefficient for electric fields ranging from 2 MV/cm ($\beta/\alpha = 218$) to 3.3 MV/cm ($\beta/\alpha = 5.26$), the electron initiated multiplication is negligible under the conditions for Fig. 2 (β/α exceeds ten for fields up to 2.98 MV/cm) [7], [9], [11]. Due to the low background doping, the electric field in the n^--GaN region changes less than 4% (as calculated by solving Poisson's equation numerically [18]) and, thus, can be treated as uniform. Under these conditions, the hole impact ionization coefficient β can be obtained as [19]:

$$\beta = \frac{\ln M_p}{W} \tag{1}$$

where W is the depletion width of the p-n junction. This analysis neglects contributions of the avalanche multiplication in the InGaN region since the electric field in the InGaN is appreciably smaller than the field in the n^--GaN region.

Fig. 3 shows the extracted hole impact ionization coefficients at 298, 348, and 398 K as a function of the inverse electric field. The hole impact ionization coefficients decrease with temperature due to the increased phonon scattering rate at elevated temperatures [20]. The data were fitted using the following equations based on the Okuto–Crowell model [21]:

$$\begin{aligned} \alpha, \beta(E, T) &= a(T) \cdot \exp\left[-\frac{b(T)}{E}\right] \\ a(T) &= a_0 \cdot (1 + c(T - T_0)) \\ b(T) &= b_0 \cdot (1 + d(T - T_0)) \end{aligned} \tag{2}$$

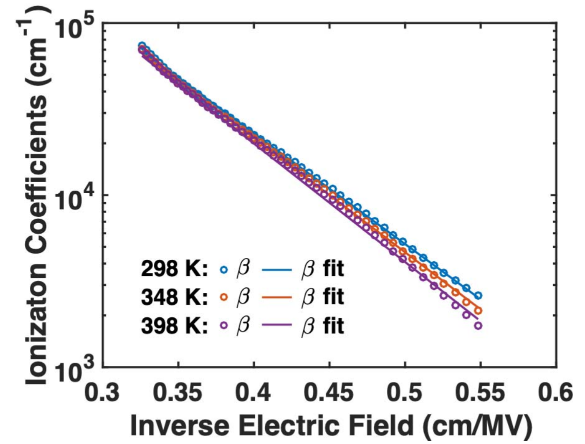

Fig. 3. Impact ionization coefficients for holes in GaN obtained from measured M_p at 298, 348, and 398 K. Points show the measured impact ionization coefficients, and solid lines represent the least-squares fits based on the Okuto–Crowell model.

where E is the electric field (V/cm) and T is the temperature in Kelvin ($T_0 = 298$ K). In the Okuto–Crowell model, the temperature-dependent coefficients $a(T)$ and $b(T)$ are linear functions of temperature, and parameters a_0, b_0, c, and d are constants. A least-squares fitting procedure was used to determine these constants for hole-initiated impact ionization:

$$\begin{aligned} a(T) &= 8.53 \times 10^6 \ \mathrm{cm}^{-1} \\ &\quad \cdot [1 + 3.23 \times 10^{-3} \ \mathrm{K}^{-1} \cdot (T - 298 \ \mathrm{K})] \\ b(T) &= 1.48 \times 10^7 \ \mathrm{V \cdot cm}^{-1} \\ &\quad \cdot [1 + 7.02 \times 10^{-4} \ \mathrm{K}^{-1} \cdot (T - 298 \ \mathrm{K})]. \end{aligned} \tag{3}$$

For the case of electrons, the low electron multiplication factor makes the extraction more sensitive to dark currents [7]. Therefore, we have also fabricated p-i-n diodes without an InGaN layer [as shown in Fig. 1(b)] to reduce the dark current and investigated the electron impact ionization coefficients using this structure. As shown in Fig. 5(a), a positive coefficient of breakdown voltage is obtained, consistent with avalanche breakdown. Fig. 4(a) shows the reverse I–V characteristics of the p-i-n diode under dark and 193-nm UV illumination at room temperature. For the data shown in Figs. 4(a) and 5(a), an incident light intensity of 2 mW/cm^2, as calibrated with a power meter, was used. As can be seen, the leakage current density is much lower than the photocurrent, leading to good extraction certainty. Due to the very short illumination wavelength, nearly pure electron injection is achieved (estimated $> 96\%$), and the electron multiplication factor can be obtained directly. The low drift layer doping (2×10^{16} cm^{-3}) results in a uniform electric field to within 4%. As with the holes, the electron multiplication factor M_n was extracted as the ratio of the measured photocurrent (including amplification) to the baseline photocurrent. The baseline photocurrent was then extrapolated into the avalanche region by extrapolating the non-avalanche contributions to reverse current with a variable-range hopping model [15]. In this model, $J_{ph,n} = J_0 + J_1 \exp(p_1 V)$, where $J_0 = 3.20 \times 10^{-4}$ A/cm^2 accounts for the diffusion photocurrent, while $J_1 = 2.23 \times 10^{-8}$ A/cm^2 and $p_1 = 8.10 \times 10^{-2}$ V^{-1}

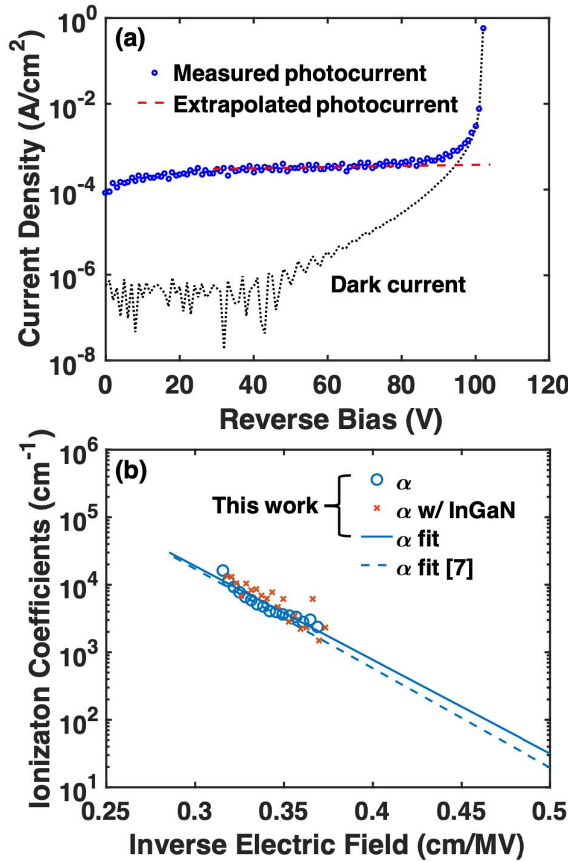

Fig. 4. (a) Reverse I–V characteristics of the p-i-n diode in Fig. 1(b) under dark and 193-nm UV illumination at room temperature. The red broken line shows the extrapolated photocurrent. (b) Impact ionization coefficients of electrons extracted from the photocurrent measurements of the p-i-n diode. Symbols show the experimentally extracted electron ionization coefficients (blue circles for extraction from p-i-n diodes without InGaN and orange crosses for devices with InGaN), and solid lines show the Chynoweth fits. The dashed line shows the Chynoweth fit for electrons obtained from devices with InGaN from our previous report [7].

account for the variable-range hopping contribution to the reverse current. These parameters were determined from least-squares fitting to the measured photocurrent from 60 to 75 V [15]–[17]. This extrapolation is shown in Fig. 4(a) by the red broken line.

The electron impact ionization coefficients α can then be extracted using the following equation [22]:

$$\alpha = \frac{1}{W}\frac{M_n - 1}{M_n - M_p}\ln\frac{M_n}{M_p}. \quad (4)$$

In (4), both electron (M_n) and hole (M_p) multiplication factors are needed to extract α, in contrast to the situation above for holes, due to the large asymmetry between electron and hole impact ionization coefficients. Hole multiplication factors (M_p) at 298 K from Fig. 2(b) were used in (4) to find α. Fig. 4(b) shows the extracted electron impact ionization coefficients of the p-i-n diode as a function of average n$^-$-GaN layer electric field. As can be seen, the extracted electron ionization coefficients are well behaved and show little scatter. For comparison, α extracted from measurements of devices, including an InGaN layer, are also shown. These data exhibit the same trend but with a larger scatter due to the higher dark current as noted previously. The Chynoweth least-squares fit for electron impact ionization coefficients at 298 K from these measurements was found to be

$$\alpha(E) = 2.77 \times 10^8\ \text{cm}^{-1} \exp(-3.20 \times 10^7\ \text{V} \cdot \text{cm}^{-1}/E). \quad (5)$$

The electron impact ionization coefficients extracted here using the p-i-n diodes are very close to previously reported data obtained using devices with an InGaN layer [7], as shown by the dashed line in Fig. 4(b). This serves both as a confirmation of previously reported values, as well as an indicator that the active regions in the device structures in Fig. 1(a) and (b) are indeed nearly identical.

The temperature dependence of the electron impact ionization coefficients has also been evaluated. Fig. 5(a) shows the reverse I–V characteristics of the p-i-n diode under dark and 193-nm UV illumination at various temperatures. As can be seen, the breakdown voltage increases with temperature, indicating avalanche breakdown. It should be noted that the breakdown voltage of the GaN-only structure in Fig. 5 is approximately 11 V lower than that of the structure including the InGaN layer (see Fig. 2), due to the increased total depletion thickness in the latter case. From the photocurrent and dark current measurements, the electron multiplication factor M_n at different temperatures can be obtained, as shown in Fig. 5(b). The hole multiplication factors M_p at different temperatures were measured using the photocurrent method from the devices with the InGaN layer, as shown in Fig. 2(b). With the electron and hole multiplication factors at different temperatures, the electron impact ionization coefficients at different temperatures were extracted according to (4). Fig. 5(c) shows the extracted electron impact ionization coefficients at 298, 348, and 398 K. The measured electron impact ionization coefficients were fitted using the Okuto–Crowell model. The parameters in the model show a linear temperature dependence, with least-squares fits resulting in

$$\begin{aligned} a(T) &= 2.77 \times 10^8\ \text{cm}^{-1} \\ &\quad \cdot [1 + 3.09 \times 10^{-3}\ \text{K}^{-1} \cdot (T - 298\ \text{K})] \\ b(T) &= 3.20 \times 10^7\ \text{V} \cdot \text{cm}^{-1} \\ &\quad \cdot [1 + 5.03 \times 10^{-4}\ \text{K}^{-1} \cdot (T - 298\ \text{K})]. \end{aligned} \quad (6)$$

The temperature dependence results of the impact ionization coefficients obtained here are in good agreement with Maeda's results; he reported $c = 1.5 \times 10^{-3}\ \text{K}^{-1}$ and $d = 6.0 \times 10^{-4}\ \text{K}^{-1}$ in (2) [10]. Due to experimental limitations, Maeda has only reported the temperature dependence of GaN's effective impact ionization coefficients with the assumption of $\alpha_{\text{eff}} \equiv \alpha = \beta$, while we have reported the temperature dependence of GaN's electron and hole impact ionization coefficients separately. The results of electrons and holes are summarized in Table I. As a consistency check, the coefficients in Table I were used to simulate the hole and electron multiplication factors as a function of average drift layer electric field for the device structures in Fig. 1. The simulated hole multiplication factor (M_p) is compared to the measured results in Fig. 2(b) and electrons (M_n) in Fig. 5(b). As can be seen, very good agreement is obtained. In addition, we observe that the temperature dependence obtained in

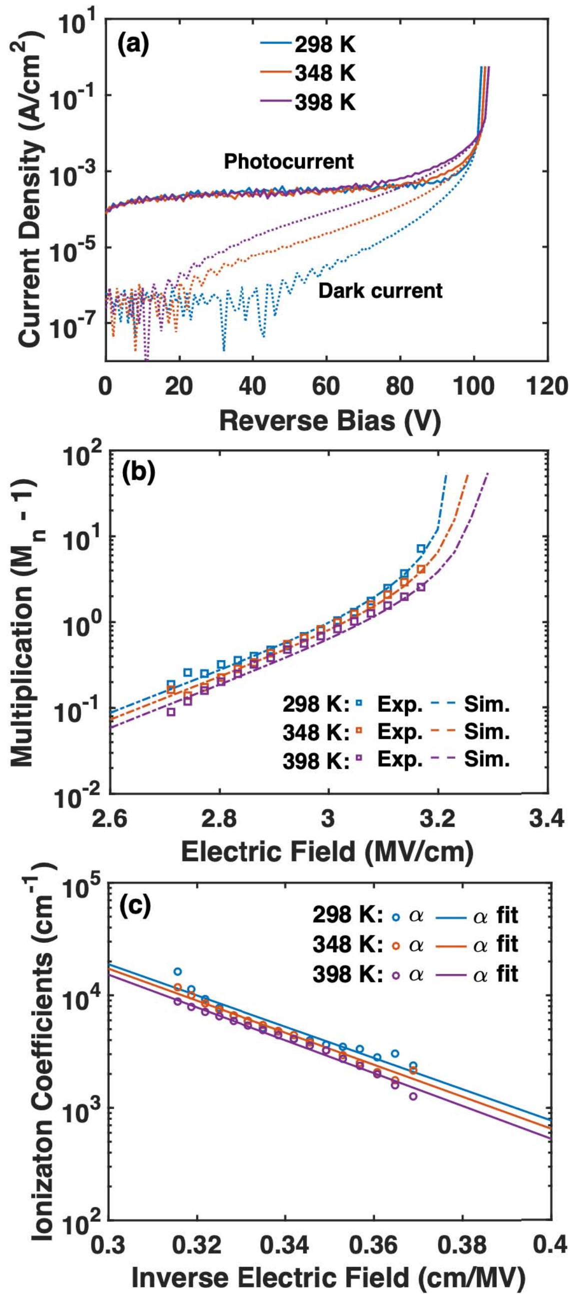

Fig. 5. (a) Reverse *I–V* characteristics of the p-i-n diode under dark and 193-nm UV illumination at various temperatures. (b) Electron multiplication factors (M_n− 1) versus electric field at various temperatures. Points show the experimental measured values, while dashed lines show the simulated values using the ionization coefficients obtained here (shown in Table I). (c) Impact ionization coefficients for electrons of GaN at 298, 348, and 398 K. Points show the measured impact ionization coefficients, and solid lines represent the least-squares fits based on the Okuto–Crowell model.

Figs. 3 and 5(c) indicates that impact ionization is a weak function of temperature for GaN. While the least-squares fit shown in Figs. 3 and 5(c) are numerically distinct (i.e., the fit lines are separated by more than the root-mean-squared error associated with each fit), as discussed in [20], the longitudinal optical (LO) phonon energy of GaN (∼92 meV) is appreciably larger than that of many other semiconductors, leading to reduced temperature dependence of the avalanche coefficients.

An important consideration for material parameter extractions is its predictive capability for structures other than those used for the extraction. To assess this, the breakdown voltage of non-punch through p-n diodes was calculated using Fulop's power law approximation for the effective impact ionization coefficients [41], [42]:

$$\alpha_{\text{eff}} = \frac{\alpha - \beta}{\ln(\alpha) - \ln(\beta)}. \quad (7)$$

For the 298 K α and β reported here, this results in

$$\alpha_{\text{eff}}(298\ \text{K}) = 6.496 \times 10^{-41} E^{6.881} \quad (8)$$

where E is in V/cm and α_{eff} is in cm^{-1}. The theoretical breakdown voltage of GaN non-punch through p-n diodes based on the effective impact ionization coefficients gives

$$\text{BV}_{298\text{K}} = 1.477 \times 10^{15} {N_D}^{-0.746} \quad (9)$$

where $\text{BV}_{298\text{ K}}$ is the breakdown voltage in V and N_D is the doping concentration (in cm^{-3}) of the drift layer. Fig. 6 shows a comparison of the breakdown voltage versus drift layer doping for a range of devices reported in the literature from a number of groups around the world, alongside the avalanche-limited theoretical breakdown voltage based on the measured coefficients. It should be noted that the positions of the data points in Fig. 6 are those reported by the respective authors; variations due to experimental technique for determining the drift layer doping or breakdown criteria, as well as edge

TABLE I
OKUTO–CROWELL MODEL PARAMETERS OF GaN'S IMPACT IONIZATION COEFFICIENTS

Parameters	Electrons (α)	Holes (β)
a_0 (cm^{-1})	2.77×10^8	8.53×10^6
b_0 (V/cm)	3.20×10^7	1.48×10^7
c (K^{-1})	3.09×10^{-3}	3.23×10^{-3}
d (K^{-1})	5.03×10^{-4}	7.02×10^{-4}
T_0 (K)	298	298

Parameters a_0, b_0, c and d are constants in the Okuto-Crowell model, obtained using the least-squares fitting method. Okuto-Crowell model is expressed as $\alpha, \beta(E,T) = a(T)\cdot\exp[-b(T)/E]$, $a(T) = a_0\cdot(1+c(T-T_0))$, $b(T) = b_0\cdot(1+d(T-T_0))$, where E is the electric field (V/cm) and T is the temperature in Kelvin.

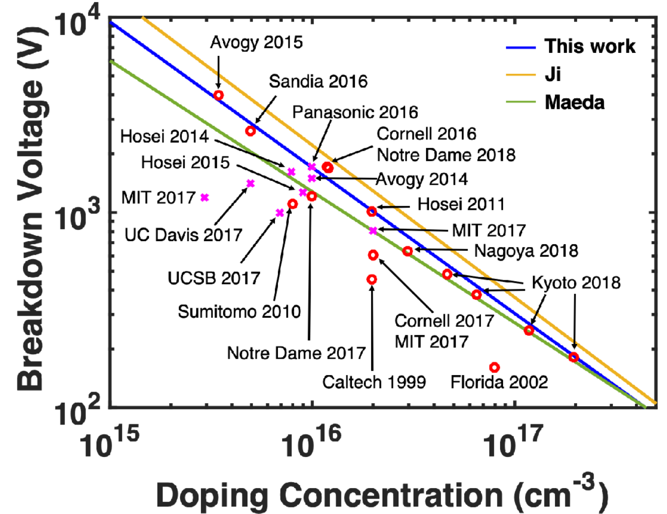

Fig. 6. Benchmark plots of breakdown voltage versus doping concentration for reported GaN power devices [(o: diodes, ×: FETs)]. The experimental data are from [2], [4], [23]–[40], and lines correspond to the predicted theoretical breakdown voltage based on measured impact ionization coefficients from Ji *et al.* [9], Maeda *et al.* [11], and this work.

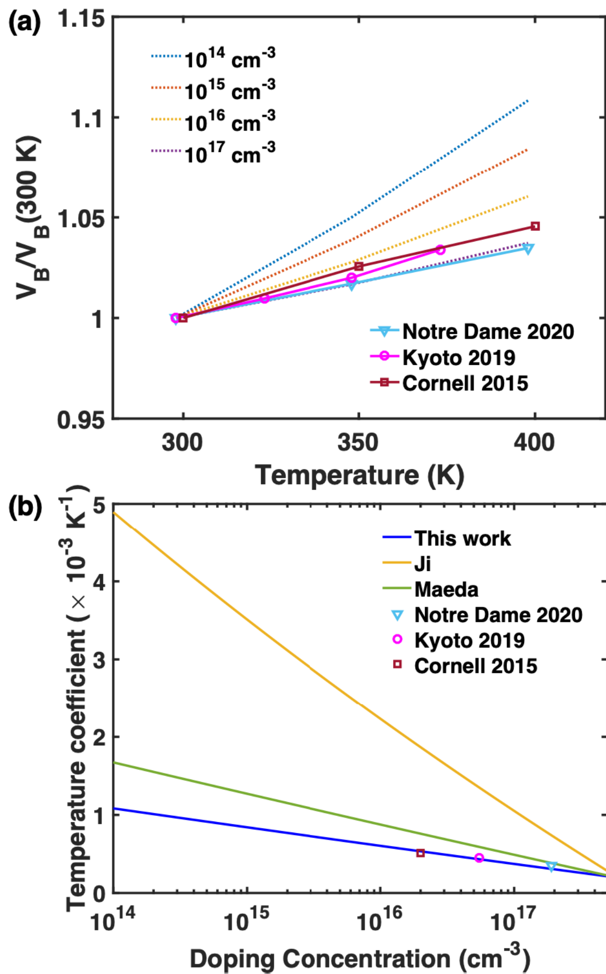

Fig. 7. (a) Normalized avalanche breakdown voltage versus temperature for GaN non-punch through p-n diodes for different n-GaN doping concentrations (N_D). (b) Theoretical breakdown voltage temperature coefficients (k) of GaN non-punch through p-n diodes versus doping concentration based on measured temperature-dependent impact ionization coefficients from Ji *et al.* [9], Maeda *et al.* [10], and this work. The symbols are measured data from different research groups. (▽: $N_D = 1.9 \times 10^{17}$ cm^{-3} [43]; ○: $N_D = 5.5 \times 10^{16}$ cm^{-3} [44]; and □: $N_D = 2 \times 10^{16}$ cm^{-3} [45].)

termination and material nonuniformity effects, may contribute to relative shifts in the positions of these points. The theoretical limits based on measured impact ionization from other groups (Ji *et al.* [9] and Maeda *et al.* [11]) are also provided for comparison. As can be seen, our model accurately bounds the experimental results from many groups—despite variations in material growth techniques, device structures, and fabrication approaches—over a wide range of both breakdown voltage and doping concentrations. This suggests that the coefficients obtained here may have wide applicability.

Using the temperature dependence of ionization coefficients, the temperature dependence of the breakdown voltage of nonpunchthrough p-n diodes was also calculated using Fulop's power law approximation. Doing so results in the following effective impact ionization coefficients at elevated temperatures:

$$\alpha_{\text{eff}}(348\text{K}) = 6.730 \times 10^{-42} E^{7.029}$$
$$\alpha_{\text{eff}}(398\text{K}) = 5.566 \times 10^{-43} E^{7.191} \quad (10)$$

where E is in V/cm and α_{eff} is in cm^{-1}. Fig. 7(a) shows the projected temperature dependence of breakdown voltage for vertical GaN nonpunchthrough p-n diodes as a function of temperature and doping concentration using the measured impact ionization coefficients. As can be seen, for drift-layer doping from 1×10^{14} cm^{-3} to 1×10^{17} cm^{-3}, the breakdown voltage increases linearly with temperature from 298 to 398 K. For the same temperature range, the predicted percentage change in breakdown voltage increases with decreasing doping concentration. The temperature dependence of breakdown voltage can be expressed as [1]:

$$\text{BV}(T) = \text{BV}_{298\text{K}}(1 + k\Delta T) \quad (11)$$

where k is the temperature coefficient. Fig. 7(b) shows the theoretical breakdown voltage temperature coefficients of GaN nonpunchthrough diodes as a function of drift layer doping concentration based on measured temperature-dependent impact ionization coefficients. Predictions based on measured impact ionization results from Ji *et al.* [9] and Maeda *et al.* [10] are also shown. As can be seen, based on our measured coefficients, the temperature coefficient for breakdown voltage increases from 3.72×10^{-4} K^{-1} to 1.08×10^{-3} K^{-1} when the doping concentration is decreased from 1×10^{17} cm^{-3} to 1×10^{14} cm^{-3}. The measured temperature-dependent BVs of GaN p-n diodes and their corresponding temperature coefficients from different research groups are shown as symbols in Fig. 7. Compared to Ji and Maeda's results, the experimental results from different research groups agree well with our calculated results, indicating that the measured temperature-dependent impact ionization coefficients may serve as a design guideline for GaN power devices at elevated temperatures.

IV. Conclusion

The breakdown and avalanche multiplication characteristics of GaN p-i-n diodes grown on native GaN substrates have been investigated. Electron and hole impact ionization coefficients for GaN epitaxial structures grown on bulk GaN substrates have been extracted using the photomultiplication method. The impact ionization coefficients of electrons and holes are also measured at elevated temperatures up to 398 K. Both the electron and hole impact ionization coefficients decrease as the temperature increases. The temperature dependence of the breakdown voltage of GaN non-punch through p-n diodes has also been predicted using the measured impact ionization coefficients. The experimentally validated impact ionization coefficients reported here may be valuable for the design of improved optoelectronic, microwave, and power devices.

References

[1] I. C. Kizilyalli, A. P. Edwards, O. Aktas, T. Prunty, and D. Bour, "Vertical power p-n diodes based on bulk GaN," *IEEE Trans. Electron Devices*, vol. 62, no. 2, pp. 414–422, Feb. 2015, doi: 10.1109/TED.2014.2360861.

[2] T. Oka, T. Ina, Y. Ueno, and J. Nishii, "1.8mΩ·cm^2 vertical GaN-based trench metal-oxide-semiconductor field-effect transistors on a free-standing GaN substrate for 1.2-kV-class operation," *Appl. Phys. Exp.*, vol. 8, no. 5, pp. 5–8, Apr. 2015, doi: 10.7567/APEX.8.054101.

[3] J. Wang *et al.*, "High voltage vertical p-n diodes with ion-implanted edge termination and sputtered SiN$_x$ passivation on GaN substrates," in *IEDM Tech. Dig.*, Dec. 2017, pp. 9.6.1–9.6.4, doi: 10.1109/IEDM.2017.8268361.

[4] T. Maeda *et al.*, "Parallel-plane breakdown fields of 2.8-3.5 MV/cm in GaN-on-GaN p-n junction diodes with double-side-depleted shallow bevel termination," in *IEDM Tech. Dig.*, Dec. 2018, pp. 18–21, doi: 10.1109/IEDM.2018.8614669.

[5] K. Kunihiro, K. Kasahara, Y. Takahashi, and Y. Ohno, "Experimental evaluation of impact ionization coefficients in GaN," *IEEE Electron Device Lett.*, vol. 20, no. 12, pp. 608–610, Dec. 1999, doi: 10.1109/55.806100.

[6] R. McClintock, J. L. Pau, K. Minder, C. Bayram, P. Kung, and M. Razeghi, "Hole-initiated multiplication in back-illuminated GaN avalanche photodiodes," *Appl. Phys. Lett.*, vol. 90, no. 14, Apr. 2007, Art. no. 141112, doi: 10.1063/1.2720712.

[7] L. Cao *et al.*, "Experimental characterization of impact ionization coefficients for electrons and holes in GaN grown on bulk GaN substrates," *Appl. Phys. Lett.*, vol. 112, no. 26, Jun. 2018, Art. no. 262103, doi: 10.1063/1.5031785.

[8] L. Cao, H. Ye, J. Wang, and P. Fay, "Avalanche multiplication noise in GaN p–n junctions grown on native GaN substrates," *Phys. Status Solidi B*, vol. 257, no. 2, Feb. 2020, Art. no. 1900373, doi: 10.1002/pssb.201900373.

[9] D. Ji, B. Ercan, and S. Chowdhury, "Experimental determination of impact ionization coefficients of electrons and holes in gallium nitride using homojunction structures," *Appl. Phys. Lett.*, vol. 115, no. 7, Aug. 2019, Art. no. 073503, doi: 10.1063/1.5099245.

[10] T. Maeda *et al.*, "Measurement of avalanche multiplication utilizing Franz-Keldysh effect in GaN p-n junction diodes with double-side-depleted shallow bevel termination," *Appl. Phys. Lett.*, vol. 115, no. 14, Sep. 2019, Art. no. 142101, doi: 10.1063/1.5114844.

[11] T. Maeda *et al.*, "Impact ionization coefficients in GaN measured by above- and sub-E_g illuminations for p^-/n^+ junction," in *IEDM Tech. Dig.*, Dec. 2019, pp. 4.2.1–4.2.4, doi: 10.1109/IEDM19573.2019.8993438.

[12] J. F. Muth *et al.*, "Absorption coefficient, energy gap, exciton binding energy, and recombination lifetime of GaN obtained from transmission measurements," *Appl. Phys. Lett.*, vol. 71, no. 18, pp. 2572–2574, Nov. 1997, doi: 10.1063/1.120191.

[13] A. Rashidi, M. Monavarian, A. Aragon, and D. Feezell, "Thermal and efficiency droop in InGaN/GaN light-emitting diodes: Decoupling multiphysics effects using temperature-dependent RF measurements," *Sci. Rep.*, vol. 9, no. 1, p. 19921, Dec. 2019, doi: 10.1038/s41598-019-56390-2.

[14] S. Shishehchi, A. Asgari, and R. Kheradmand, "The effect of temperature on the recombination rate of AlGaN/GaN light emitting diodes," *Opt. Quantum Electron.*, vol. 41, no. 7, pp. 525–530, May 2009, doi: 10.1007/s11082-009-9353-7.

[15] Y. Zhang *et al.*, "Design space and origin of off-state leakage in GaN vertical power diodes," in *IEDM Tech. Dig.*, Dec. 2015, pp. 35.1.1–35.1.4, doi: 10.1109/IEDM.2015.7409830.

[16] S. M. Sze and K. K. Ng, *Physics of Semiconductor Devices*. Hoboken, NJ, USA: Wiley, 2006.

[17] M. Musolino *et al.*, "A physical model for the reverse leakage current in (in,Ga)N/GaN light-emitting diodes based on nanowires," *J. Appl. Phys.*, vol. 119, no. 4, Jan. 2016, Art. no. 044502, doi: 10.1063/1.4940949.

[18] G. L. Snider, I.-H. Tan, and E. L. Hu, "Electron states in mesa-etched onedimensional quantum well wires," *J. Appl. Phys.*, vol. 68, no. 6, pp. 2849–2853, Sep. 1990, doi: 10.1063/1.346443.

[19] H. Niwa, J. Suda, and T. Kimoto, "Impact ionization coefficients in 4H-SiC toward ultrahigh-voltage power devices," *IEEE Trans. Electron Devices*, vol. 62, no. 10, pp. 3326–3333, Oct. 2015, doi: 10.1109/TED.2015.2466445.

[20] L. Tirino, M. Weber, K. F. Brennan, E. Bellotti, and M. Goano, "Temperature dependence of the impact ionization coefficients in GaAs, cubic SiC, and zinc-blende GaN," *J. Appl. Phys.*, vol. 94, no. 1, pp. 423–430, Jul. 2003, doi: 10.1063/1.1579129.

[21] Y. Okuto and C. R. Crowell, "Threshold energy effect on avalanche breakdown voltage in semiconductor junctions," *Solid-State Electron.*, vol. 18, no. 2, pp. 161–168, Feb. 1975, doi: 10.1016/0038-1101(75)90099-4.

[22] C. A. Lee, R. A. Logan, R. L. Batdorf, J. J. Kleimack, and W. Wiegmann, "Ionization rates of holes and electrons in silicon," *Phys. Rev.*, vol. 134, no. 3, pp. A761–A773, May 1964, doi: 10.1103/PhysRev.134.A761.

[23] Z. Z. Bandic *et al.*, "High voltage (450 V) GaN Schottky rectifiers," *Appl. Phys. Lett.*, vol. 74, no. 9, pp. 1266–1268, Mar. 1999, doi: 10.1063/1.123520.

[24] J. W. Johnson *et al.*, "Breakdown voltage and reverse recovery characteristics of free-standing GaN Schottky rectifiers," *IEEE Trans. Electron Devices*, vol. 49, no. 1, pp. 32–36, Jan. 2002, doi: 10.1109/16.974745.

[25] Y. Saitoh *et al.*, "Extremely low on-resistance and high breakdown voltage observed in vertical GaN Schottky barrier diodes with high-mobility drift layers on low-dislocation-density GaN substrates," *Appl. Phys. Exp.*, vol. 3, no. 8, Jul. 2010, Art. no. 081001, doi: 10.1143/APEX.3.081001.

[26] W. Li *et al.*, "Design and realization of GaN trench junction-barrier-Schottky-Diodes," *IEEE Trans. Electron Devices*, vol. 64, no. 4, pp. 1635–1641, Apr. 2017, doi: 10.1109/TED.2017.2662702.

[27] Y. Zhang *et al.*, "Vertical GaN junction barrier Schottky rectifiers by selective ion implantation," *IEEE Electron Device Lett.*, vol. 38, no. 8, pp. 1097–1100, Aug. 2017, doi: 10.1109/LED.2017.2720689.

[28] K. Nomoto, Y. Hatakeyama, H. Katayose, N. Kaneda, T. Mishima, and T. Nakamura, "Over 1.0 kV GaN p -n junction diodes on free-standing GaN substrates," *Phys. Status Solidi A*, vol. 208, no. 7, pp. 1535–1537, Jul. 2011, doi: 10.1002/pssa.201000976.

[29] Y. Zhang *et al.*, "Novel GaN trench MIS barrier Schottky rectifiers with implanted field rings," in *IEDM Tech. Dig.*, Dec. 2016, pp. 10.2.1–10.2.4, doi: 10.1109/IEDM.2016.7838386.

[30] K. Nomoto *et al.*, "1.7-kV and 0.55-m$\Omega \cdot cm^2$ GaN p-n diodes on bulk GaN substrates with avalanche capability," *IEEE Electron Device Lett.*, vol. 37, no. 2, pp. 161–164, Feb. 2016, doi: 10.1109/LED.2015.2506638.

[31] O. Aktas and I. C. Kizilyalli, "Avalanche capability of vertical GaN p-n junctions on bulk GaN substrates," *IEEE Electron Device Lett.*, vol. 36, no. 9, pp. 890–892, Sep. 2015, doi: 10.1109/LED.2015.2456914.

[32] J. R. Dickerson *et al.*, "Vertical GaN power diodes with a bilayer edge termination," *IEEE Trans. Electron Devices*, vol. 63, no. 1, pp. 419–425, Jan. 2016, doi: 10.1109/TED.2015.2502186.

[33] S. Usami *et al.*, "Correlation between dislocations and leakage current of p-n diodes on a free-standing GaN substrate," *Appl. Phys. Lett.*, vol. 112, no. 18, Apr. 2018, Art. no. 182106, doi: 10.1063/1.5024704.

[34] T. Oka, Y. Ueno, T. Ina, and K. Hasegawa, "Vertical GaN-based trench metal oxide semiconductor field-effect transistors on a free-standing GaN substrate with blocking voltage of 1.6 kV," *Appl. Phys. Exp.*, vol. 7, no. 2, pp. 8–11, Jan. 2014, doi: 10.7567/APEX.7.021002.

[35] H. Nie *et al.*, "1.5-kV and 2.2-mΩ-cm^2 vertical GaN transistors on bulk-GaN substrates," *IEEE Electron Device Lett.*, vol. 35, no. 9, pp. 939–941, Sep. 2014, doi: 10.1109/LED.2014.2339197.

[36] D. Shibata *et al.*, "1.7 kV/1.0 mΩcm^2 normally-off vertical GaN transistor on GaN substrate with regrown p-GaN/AlGaN/GaN semipolar gate structure," in *IEDM Tech. Dig.*, Dec. 2016, pp. 10.1.1–10.1.4, doi: 10.1109/IEDM.2016.7838385.

[37] M. Sun, Y. Zhang, X. Gao, and T. Palacios, "High-performance GaN vertical fin power transistors on bulk GaN substrates," *IEEE Electron Device Lett.*, vol. 38, no. 4, pp. 509–512, Apr. 2017, doi: 10.1109/LED.2017.2670925.

[38] C. Gupta *et al.*, "*In situ* oxide, GaN interlayer-based vertical trench MOSFET (OG-FET) on bulk GaN substrates," *IEEE Electron Device Lett.*, vol. 38, no. 3, pp. 353–355, Mar. 2017, doi: 10.1109/LED.2017.2649599.

[39] D. Ji *et al.*, "Demonstrating >1.4 kV OG-FET performance with a novel double field-plated geometry and the successful scaling of large-area devices," in *IEDM Tech. Dig.*, Dec. 2017, pp. 9.4.1–9.4.4, doi: 10.1109/IEDM.2017.8268359.

[40] J. Wang *et al.*, "High voltage, high current GaN-on-GaN p-n diodes with partially compensated edge termination," *Appl. Phys. Lett.*, vol. 113, no. 2, Jul. 2018, Art. no. 023502, doi: 10.1063/1.5035267.

[41] W. Fulop, "Calculation of avalanche breakdown voltages of silicon p-n junctions," *Solid-State Electron.*, vol. 10, no. 1, pp. 39–43, Jan. 1967, doi: 10.1016/0038-1101(67)90111-6.

[42] Z. Li, V. Pala, and T. P. Chow, "Avalanche breakdown design parameters in GaN," *Jpn. J. Appl. Phys.*, vol. 52, no. 8, May 2013, Art. no. 08JN05, doi: 10.7567/JJAP.52.08JN05.

[43] L. Cao, "GaN-based impact-ionization avalanche transit-time (IMPATT) diodes and low-loss interconnects for microwave and millimeter wave applications," Ph.D. dissertation, Dept. Elect. Eng., Univ. Notre Dame, Notre Dame, IN, USA, 2020.

[44] T. Maeda *et al.*, "Design and fabrication of GaN p-n junction diodes with negative beveled-mesa termination," *IEEE Electron Device Lett.*, vol. 40, no. 6, pp. 941–944, Jun. 2019, doi: 10.1109/LED.2019.2912395.

[45] Z. Hu *et al.*, "Near unity ideality factor and Shockley-Read-Hall lifetime in GaN-on-GaN p-n diodes with avalanche breakdown," *Appl. Phys. Lett.*, vol. 107, no. 24, Dec. 2015, Art. no. 243501, doi: 10.1063/1.4937436.